

Kondo Tunneling into a Quantum Spin Hall Insulator

Igor Kuzmenko, Anatoly Golub and Yshai Avishai

Department of Physics, Ben-Gurion University of the Negev Beer-Sheva, Israel

(Dated: November 17, 2018)

The physics of a junction composed of a normal metal, quantum dot and 2D topological insulator (in a quantum spin Hall state) is elucidated. It manifests a subtle combination of Kondo correlations and quantum spin Hall edge states moving on the opposite sides of the 2D topological insulator. In a narrow strip geometry these edge states interact and a gap opens in the edge state spectrum. Consequently, Kondo screening is less effective and that affects electron transport through the junction. Specifically, when edge state coupling is strong enough, the tunneling differential conductance develops a dip at zero temperature instead of the standard zero bias Kondo peak.

PACS numbers: 71.10.Pm, 73.43.-f, 72.15.Qm, 73.23.-b

Background: Topological insulators (TI) and topological superconductors (TS) have recently become a subject of intense theoretical and experimental studies.^{1–14} In most of these studies, properties of topological states are analyzed using classification of the electronic phases according to the pertinent topological invariants.^{1–8}

Two-dimensional TI are systems in which time reversal symmetry is respected but spin rotation invariance is violated. They differ from ordinary insulators as they possess a non-trivial topological number Z_2 implying a gapped spectrum in the bulk and gapless spectrum of quantum spin Hall (QSH) edge states¹⁵ (or helical modes). A helical mode consists of a Kramers degenerate pair of states propagating in opposite directions along the same edge. Elucidating the QSH helical modes in experiments is rather elusive since both edge states moving on opposite boundaries contribute to the conductance.¹⁶ This obstacle can be alleviated if there are strong correlations of edge states on the opposite edges, leading to the emergence of massive Dirac fermions instead of the massless ones that prevail in the absence of such correlations.

Motivation: In order to employ this feature, we note that the physics of QSH state can be studied in tunneling experiments.^{17–23} In particular, we focus on tunneling through an interacting quantum dot tuned to the Kondo regime. In the absence of correlations between edge states, Kondo tunneling into a TI with gapless helical edge state spectrum displays a finite zero bias differential conductance at zero temperature²³, as is the case for tunneling into a metal. Once the coupling between the helical states on the opposite sides of the TI is present, a gap opens in the edge states spectrum, which naturally affects the tunneling conductance.¹⁶ Screening of the magnetic impurity becomes less effective and the conductance develops a dip at zero temperature.

The main objective: The main goal of the present work is to substantiate the above qualitative analysis. It is argued that interaction between QSH edge states on a 2D TI has a clear signature that turns it to be experimentally detectable as it leads to unusual behavior of Kondo tunneling at zero temperature.

Main results: We have theoretically analyzed tunneling through a device consisting of a tunnel junction com-

posed of normal metal (NM) interacting quantum dot (QD) and 2D TI as shown in Fig. 1. The TI is modeled as a stripe with topological states moving on its opposite sides with a coupling between them. Interrelation between the Kondo physics prevailing in the QD and the QSH physics prevailing in the TI is then studied. Kondo tunneling is analyzed in the weak ($T \gg T_K$) and strong ($T < T_K$) coupling regimes, where T_K is a Kondo temperature. It is shown that in both regimes, the conductance develops a dip when the temperature T decreases and crosses an energy threshold ν specifying the coupling strength between the QSH edge states. Since this setup is experimentally feasible we argue that coupling between QSH edge states residing on opposite edges of a 2D TI has a definite experimental signature.

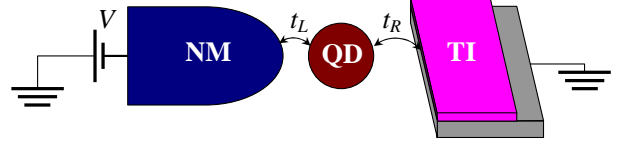


FIG. 1: NM-QD-TI junction. Helical states exist on the edges of the TI. The QD can be gated to adjust the level position in the dot and/or the tunneling rates t_L and t_R .

Anderson Model for NM-QD-TI Junction: The junction consists of the following ingredients (see Fig. 1): the NM lead, held at bias voltage V ; the TI with coupling between helical modes on its two opposite sides; the QD in a tunnel contact with the NM and with the TI. The Hamiltonian of the junction is then written as,

$$H = H_L + H_R + H_D + H_T. \quad (1)$$

The first term on the right hand side of Eq. (1) is the Hamiltonian of the NM lead,

$$H_L = \sum_{\mathbf{k}\sigma} \epsilon_{\mathbf{k}} c_{\mathbf{k}\sigma}^\dagger c_{\mathbf{k}\sigma}. \quad (2)$$

The second term, H_R , is the low energy Hamiltonian of the 2D TI,

$$H_R = \hbar \sum_{k\sigma r} v_{\sigma r} k \alpha_{k\sigma r}^\dagger \alpha_{k\sigma r} + \nu \sum_{k\sigma} \left[\alpha_{k\sigma 1}^\dagger \alpha_{k\sigma 2} + \text{h.c.} \right], \quad (3)$$

where ν is the coupling strength between the helical fermions on the opposite sides ($r = 1, 2$) of the TI, and $v_{\sigma r} \equiv (-1)^{r-1} \sigma v$, with v being the Fermi velocity.

The coupling ν represents the effective mass of Dirac fermions. It is convenient to work in a basis for which the TI Hamiltonian (3) is diagonal, obtained through the canonical transformations,

$$\begin{aligned} \alpha_{k\sigma 1} &= U_k \gamma_{k\sigma+} - \sigma V_k \gamma_{k\sigma-}, \\ \alpha_{k\sigma 2} &= \sigma V_k \gamma_{k\sigma+} + U_k \gamma_{k\sigma-}, \end{aligned} \quad (4)$$

where

$$\begin{aligned} U_k &= \sqrt{\frac{\varepsilon_k + \hbar v k}{2\varepsilon_k}}, \quad V_k = \sqrt{\frac{\varepsilon_k - \hbar v k}{2\varepsilon_k}}, \\ \varepsilon_k &= \sqrt{(\hbar v k)^2 + \nu^2}. \end{aligned}$$

The Hamiltonian (3) then takes the form,

$$H_R = \sum_{k\sigma, p=\pm} p \sigma \varepsilon_k \gamma_{k\sigma p}^\dagger \gamma_{k\sigma p}. \quad (5)$$

The third term on the right hand side of Eq. (1), H_D , is the QD Hamiltonian,

$$H_D = \epsilon_0 \sum_{\sigma} d_{\sigma}^\dagger d_{\sigma} + U n_{\downarrow} n_{\uparrow}. \quad (6)$$

Here $d_{\sigma}^\dagger, d_{\sigma}$ are creation and annihilation operators for the dot electrons; $n_{\sigma} = d_{\sigma}^\dagger d_{\sigma}$, and $U > 0$ is the strength of the Coulomb repulsion. The last term on the right hand side of Eq. (1), $H_T = H_{TL} + H_{TR}$, is composed of H_{TL} , describing electron tunneling between the dot and the normal metal lead, and H_{TR} describing electron tunneling between the dot and the TI.

Denoting by $\psi_L(\mathbf{r})$ and $\psi_R(\mathbf{r})$ the electron field operators in the NM and the TI and assuming the dot is positioned at $\mathbf{r} = 0$, we have,

$$\begin{aligned} H_{TL} &= t_L \sum_{\sigma} \left[\psi_{L\sigma}^\dagger(0) d_{\sigma} + \text{h.c.} \right], \\ H_{TR} &= t_R \sum_{\sigma} \left[\psi_{R\sigma}^\dagger(0) d_{\sigma} + \text{h.c.} \right], \end{aligned} \quad (7)$$

where $t_{L,R}$ are the corresponding tunneling amplitudes assumed to be spin independent.

The Spin Hamiltonian: The quantum dot is tuned by gate voltage to have a single electron in its ground state. The depth $|\epsilon_0|$ of the dot level is assumed to be much larger than the tunneling width,

$$\Gamma = \Gamma_L + \Gamma_R, \quad \Gamma_L = 2\pi t_L^2 \rho_L, \quad \Gamma_R = 2\pi t_R^2 \rho_R, \quad (8)$$

where ρ_L is the electron density of states in the NM, while ρ_R is the electron density of states belonging to the gapless part of the TI. Hence, charge fluctuations can be integrated out using the Schrieffer-Wolff transformation²⁴. It projects out zero and two electron states in the dot and maps the Hamiltonian H , Eq. (1) onto an effective

spin Hamiltonian \tilde{H} acting in a subspace of states where there is one and only one electron on the dot. The effective Hamiltonian in this subspace reads,

$$H_K = \sum_{\alpha\alpha'\sigma\sigma'} \psi_{\alpha\sigma}^\dagger(0) h_{\alpha\alpha'}^{\sigma\sigma'} \psi_{\alpha'\sigma'}(0), \quad (9)$$

where $\alpha, \alpha' = L, R$, and the matrix $h_{\alpha\alpha'}^{\sigma\sigma'}$ is defined as,

$$h_{\alpha\alpha'}^{\sigma\sigma'} = \frac{1}{4} K_{\alpha\alpha'} \delta_{\sigma\sigma'} + \frac{1}{2} J_{\alpha\alpha'} \mathbf{S} \cdot \boldsymbol{\tau}_{\sigma\sigma'}.$$

Here $\boldsymbol{\tau}$ is the vector of the Pauli matrices and \mathbf{S} is the spin operator of the electron residing on the QD. The coupling constants are

$$J_{\alpha\alpha'} = \frac{2t_{\alpha}t_{\alpha'}}{|\epsilon_0|} + \frac{2t_{\alpha}t_{\alpha'}}{U - |\epsilon_0|}, \quad K_{\alpha\alpha'} = \frac{2t_{\alpha}t_{\alpha'}}{|\epsilon_0|} - \frac{2t_{\alpha}t_{\alpha'}}{U - |\epsilon_0|}.$$

Scaling Equations Using the poor man's scaling technique, we obtain scaling equations for the dimensionless coupling constants $j_{\alpha\alpha'} = J_{\alpha\alpha'} \sqrt{\rho_{\alpha}\rho_{\alpha'}}$,

$$\frac{dj_{LL}}{d \ln D} = -(j_{LL}^2 + j_{LR}^2), \quad (10)$$

$$\frac{dj_{RR}}{d \ln D} = -(j_{RR}^2 + j_{LR}^2), \quad (11)$$

$$\frac{dj_{LR}}{d \ln D} = -j_{LR} (j_{LL} + j_{RR}), \quad (12)$$

subject to the initial conditions,

$$j_{\alpha\alpha'}(\bar{D}) = \frac{\sqrt{\Gamma_{\alpha}\Gamma_{\alpha'}}}{\pi} \left(\frac{1}{|\epsilon_0|} + \frac{1}{U - |\epsilon_0|} \right).$$

If ν is the smallest energy scale, the solutions of these equations are,

$$j_{\alpha\alpha'}(T) = \frac{\sqrt{\Gamma_{\alpha}\Gamma_{\alpha'}}}{\Gamma} \frac{1}{\ln(T/T_K)}, \quad (13)$$

and the scaling invariant, (the Kondo temperature), is

$$T_K = \bar{D} \exp \left\{ -\frac{\pi|\epsilon_0|}{\Gamma} \right\}. \quad (14)$$

When ν is not the smallest energy scale, the scaling behavior is more complicated. The flow diagram still has a fixed point at infinity, but the Kondo temperature turns out to be a sharp function of ν .^{25,26} For $\nu \gg T_K$, the scaling of $j_{\alpha\alpha'}(T)$ depends on whether the temperature is higher or lower than ν . For $T \gg \nu \gg T_K$, the gap in the edge state spectrum can be neglected and the scaling of $j_{\alpha\alpha'}(T)$ are given by Eq. (13) with the scaling invariant T_K , Eq. (14). For $\nu \gg T_K > T$ the scaling of j_{LR} and j_{RR} terminates at $D \simeq \nu$ and for $D < \nu$ we have just one scaling equation, leading to a fixed point at $j_{LL} \rightarrow \infty$ and a Kondo temperature that depends on ν . However, we will see that the tunneling conductance diminishes in the low temperature regime, $T \ll \nu$. Therefore in the

following discussions we may speak of a single Kondo temperature, given by Eq. (14).

Calculations of the Tunneling Conductance in the Weak Coupling Regime are carried out below using the Keldysh technique in order to treat a system out of equilibrium. The required quantities to be used elsewhere below are the Keldysh Green's functions (GF)

$$\bar{g}_\alpha = \begin{pmatrix} \bar{g}_\alpha^L & \bar{g}_\alpha^K \\ 0 & \bar{g}_\alpha^A \end{pmatrix}, \quad (15)$$

where the subscript α refers to the normal metal (L) and TI (R) or the dot (f) electron GF while the superscripts refer to retarded (R), advanced (A) and Keldysh (K) types of the GF. For $\alpha = L, R$ the explicit expressions are,

$$\begin{aligned} \bar{g}_L^R &= -\bar{g}_L^A = -i\pi\rho_L, & \bar{g}_L^K(\epsilon) &= -2i\pi\rho_L(1 - 2f(\epsilon)), \\ \bar{g}_R^{R,A}(\epsilon) &= -\pi\rho_R \chi(\epsilon \pm i\eta), & & \\ \bar{g}_R^K(\epsilon) &= -2i\pi\rho_R \text{Im}\chi(\epsilon) (1 - 2f(\epsilon)), & & \end{aligned} \quad (16)$$

where $f(\epsilon)$ is the Fermi function and

$$\chi(z) = \frac{iz}{\sqrt{z^2 - \nu^2}}. \quad (17)$$

The current operator for tunnelling from the NM to the TI is

$$I = \frac{ie}{\hbar} \sum_{\sigma\sigma'} \left\{ \psi_{L\sigma}^\dagger(0) h_{LR}^{\sigma\sigma'} \psi_{R\sigma'}(0) - \text{h.c.} \right\}, \quad (18)$$

and the differential dc conductance is given by,

$$G = \frac{\partial \mathcal{I}(V)}{\partial V},$$

where the expectation value of the current is

$$\mathcal{I}(V) = \langle U_K^{-1} \mathcal{T}(U_K I(0)) \rangle. \quad (19)$$

In this expression, \mathcal{T} is the time-ordering operator and U_K is the evolution operator under H_K ,

$$U_K = \mathcal{T} \exp \left\{ -\frac{i}{\hbar} \int_{-\infty}^{\infty} dt H_K(t) \right\}. \quad (20)$$

To lowest (second) non-vanishing order of perturbation theory in the dimensionless parameters $j_{\alpha\alpha'}$ and $k_{\alpha\alpha'} = K_{\alpha\alpha'}\sqrt{\rho_\alpha\rho_{\alpha'}}$, the conductance is

$$G_2 = \frac{\pi e^2}{4\hbar} \left\{ k_{LR}^2 + 3j_{LR}^2 \right\} W(T, V), \quad (21)$$

where $W(T, V) = w(T, V) + w(T, -V)$,

$$w(T, V) = \frac{1}{4T} \int_{\nu}^{\infty} \frac{\epsilon d\epsilon}{\sqrt{\epsilon^2 - \nu^2}} \frac{1}{\cosh^2\left(\frac{\epsilon + eV}{2T}\right)}.$$

The third order correction to the conductance is

$$G_3 = \frac{3\pi e^2}{2\hbar} j_{LR}^2 W(T, V) \sum_{\alpha=L,R} j_{\alpha\alpha} \mathcal{L}_\alpha(\bar{D}), \quad (22)$$

where \bar{D} is a high energy cut off,

$$\begin{aligned} \mathcal{L}_L(\bar{D}) &= \frac{1}{2} \left\{ \ln \left(\frac{\bar{D}}{\sqrt{(\nu + eV)^2 + T^2}} \right) + \right. \\ &\quad \left. + \ln \left(\frac{\bar{D}}{\sqrt{(\nu - eV)^2 + T^2}} \right) \right\}, \\ \mathcal{L}_R(\bar{D}) &= \ln \left(\frac{\bar{D}}{\sqrt{\nu^2 + T^2}} \right). \end{aligned}$$

The third order correction G_3 contains a logarithmic term which is, strictly speaking, not small. As a result, G_3 is not small compared with G_2 and the expansion up to terms cubic in $j_{\alpha\alpha'}$ is insufficient. Instead, we derive the conductance in the leading logarithmic approximation using the RG equations (10) – (12).

In the following analysis we split the second order contribution to the conductance, Eq. (21), in two parts: one part is due to the exchange cotunneling, which is proportional to j_{LR}^2 ; and one part is due to regular cotunneling, which is proportional to k_{LR}^2 . G_3 , Eq. (22), increases when the temperature and voltage are lowered, demonstrating the Kondo anomaly. The regular cotunneling contribution contains k_{LR}^2 which does not grow at low temperatures and bias, and therefore it does not contribute to the Kondo effect. The exchange cotunneling contains term j_{LR}^2 which demonstrates logarithmic enhancement of the conductance at low temperatures [see Eq. (13)] and contributes to the Kondo effect. Therefore, we single out the exchange contribution in the second order term,

$$G_2^{\text{exch}}(D) = \frac{3\pi e^2}{4\hbar} j_{LR}^2(D) W(T, V). \quad (23)$$

The resulting condition of invariance of the conductance under the transformation, which corresponds to “poor man’s scaling”, has the form,

$$\begin{aligned} \frac{\partial}{\partial \ln D} \left\{ G_2^{\text{exch}}(D) + \right. \\ \left. + \frac{3\pi e^2}{2\hbar} j_{LR}^2 W(T, V) \sum_{\alpha=L,R} j_{\alpha\alpha} \mathcal{L}_\alpha(D) \right\} = 0. \end{aligned} \quad (24)$$

Within the accuracy of this equation, when differentiating the second term, we should neglect any implicit dependence on D through the couplings $j_{\alpha\alpha'}$. Eq. (24) yields the scaling equation (12).

The renormalization procedure should proceed until the bandwidth D is reduced to a quantity $d(T, V, \nu) = \text{Mx}[T, eV, \nu]$. At this point, the third order

correction to the conductance is much smaller than G_2^{exch} and the current and conductance can be calculated in the Born approximation, as in Eq. (23). This situation is similar to the problem considered in Ref.²⁷, but the coupling between the helical modes in the TI introduces an additional energy scale ν which affects the Kondo physics. When D reduces below ν , renormalization of both j_{LR} and j_{RR} stops. Then, taking

$$d(T, V, \nu) = \sqrt{\nu^2 + (eV)^2 + T^2},$$

we get an expression for the conductance for $T, |eV| \geq T_K$,

$$G(T, V) = \frac{3\pi^2 G_0}{16} \frac{W(T, V)}{\ln^2(d(T, V, \nu)/T_K)}, \quad (25)$$

where

$$G_0 = \frac{e^2}{\pi\hbar} \frac{4\Gamma_L\Gamma_R}{(\Gamma_L + \Gamma_R)^2}.$$

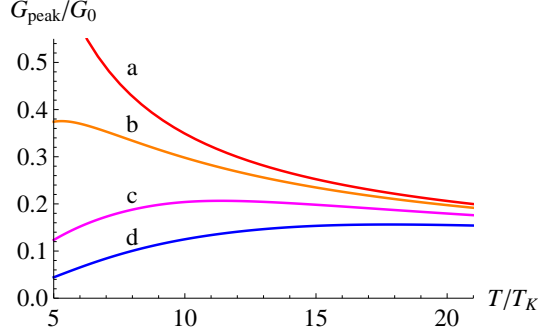


FIG. 2: Conductance as function of temperature in the weak coupling regime. The curves a, b, c and d correspond to $\nu = 0, 5T_K, 10T_K$ and $15T_K$, respectively. The case $\nu = 0$ corresponds to the standard Kondo effect in NM-QD-NM junction.²⁷

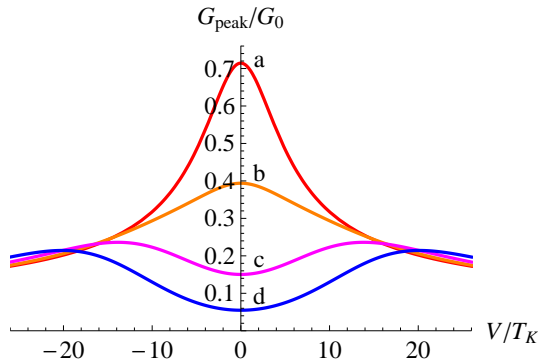


FIG. 3: The nonlinear conductance (25) as a function of applied bias for $T = 5T_K$. The curves a, b, c and d correspond to $\nu = 0, 5T_K, 10T_K$ and $15T_K$, respectively

The total differential conductance is displayed in Fig. 2 for $V = 0$. It is seen that when the gap in the spectrum

of the TI exceeds T_K (see curves b, c and d), the conductance increases when the temperature is lowered, reaches its peak at finite temperature and begins to decrease with further lowering the temperature. This occurs because electron needs an extra energy in order to overcome the gap ν between the Fermi level of the left lead and the bottom of the conduction band of the TI. This energy can be transferred from the internal energy of the electron liquid in the lead and/or from the voltage difference across the barrier. When the temperature is lower than the gap, the zero bias conductance decreases with temperature. For comparison, it is noticed that the conductance for the gapless spectrum of the TI (curve a) increases when the temperature is lowered which corresponds to the standard feature of Kondo tunneling through the NM-QD-NM junction.²⁷

The coupling between the helical states manifests itself also in the nonlinear tunneling conductance. Fig. 3 displays the nonlinear conductance as a function of the applied voltage for $T = 5T_K$ and for several values of ν . The zero bias peak in the conductance corresponding to the standard Kondo tunneling decreases with the coupling energy ν (curves a and b) and splits into two distinct peaks when ν exceeds the temperature T (curves c and d). This is one of the central results of the present paper since it combines the Kondo and the QSH physics.

Conductance Calculations in the Strong Coupling Regime: When $T < T_K$, the mean field slave boson approximation (MFSBA) is used to calculate the zero bias tunneling conductance. In the limit $U \rightarrow \infty$, the dot can be empty or singly occupied. The dot operators are written as $d_\sigma = b^\dagger f_\sigma$ and $d_\sigma^\dagger = f_\sigma^\dagger b$ where the slave fermion operators f_σ and the slave boson operator b satisfy constraint condition,

$$Q = \sum_\sigma f_\sigma^\dagger f_\sigma + b^\dagger b = 1.$$

This condition is encoded by including a Lagrange multiplier λ in the total action S . In the mean field approximation, we replace the Bose operators b and b^\dagger by their expectation values,

$$b \rightarrow b_0, \quad b^\dagger \rightarrow b_0, \quad b_0 = \sqrt{\langle b^\dagger b \rangle}.$$

At the mean field level the constraint condition is satisfied only on the average.

The partition function $Z(\alpha)$ is calculated by integrating the action over slave fermion field. Here the source field α is coupled to the current operator,

$$I = \frac{iet_L}{\hbar} \sum_\sigma [\psi_{L\sigma}^\dagger(0) b^\dagger f_\sigma - \text{h.c.}]. \quad (26)$$

The effective action in the MFSBA is Gaussian and depends on two real numbers, the boson field b_0 and the chemical potential (Lagrange multiplier) λ . Integrating the action leads to the partition function,

$$\ln Z(\alpha) = -\text{tr} \ln \left\{ G_f^{-1} - \frac{e\alpha_q t_L^2 b_0^2}{\hbar} [\bar{g}_L, \tau_x] \right\}, \quad (27)$$

where

$$G_f^{-1} = g_f^{-1} - t_L^2 b_0^2 \bar{g}_L - t_R^2 b_0^2 \bar{g}_R. \quad (28)$$

Here g_f is the GF of the (non-interacting) electron in the QD with shifted energy level, $\epsilon_0 \rightarrow \bar{\epsilon}_0 = \epsilon_0 + \lambda$,

$$g_f^{R/A}(\epsilon) = \frac{1}{\epsilon - \bar{\epsilon}_0 \pm i\eta}, \quad g_f^K(\epsilon) = -\frac{2i\eta(1 - 2f(\epsilon))}{(\epsilon - \bar{\epsilon}_0)^2 + \eta^2},$$

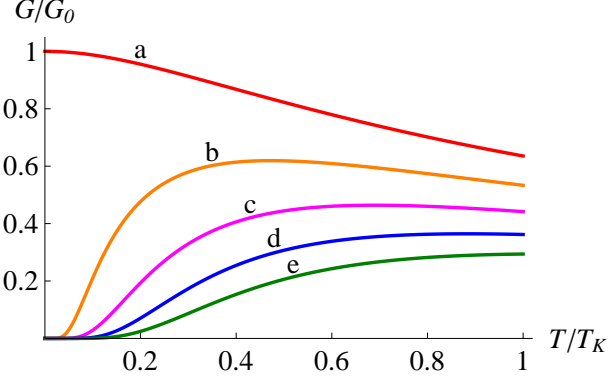


FIG. 4: The zero bias conductance as a function of temperature in the strong coupling limit ($T < T_K$). The curves a, b, c, d and e correspond to $\nu = 0, 0.2T_K, 0.4T_K, 0.6T_K$ and $0.8T_K$, respectively. Here we take $\Gamma_L = \Gamma_R$.

The MFSBA is reliable in equilibrium, $V = 0$. Therefore we will consider below the temperature dependence of the zero bias conductance. In equilibrium, the mean field solutions for b_0 and λ minimize the free energy,

$$F = -T \sum_{\omega_n} \text{tr} \ln G_f^{-1}(i\omega_n) + \lambda b_0^2,$$

where the last term is the slave boson kinetic part of the free energy due to the constraint, $G_f^{-1}(i\omega_n)$ is the Matsubara's GF. The mean field equations are

$$b_0^2 = \frac{2}{\pi} \arctan\left(\frac{2(\epsilon_0 + \lambda)}{b_0^2 \Gamma}\right), \quad \lambda = \frac{\Gamma}{\pi} \ln\left(\frac{\pi \bar{D}}{b_0^2 \Gamma}\right). \quad (29)$$

These equations are solved for b_0 and λ with the solutions,

$$b_0^2 = \frac{\pi T_K}{\Gamma}, \quad \epsilon_0 + \lambda = \frac{\pi^3 (T_K)^2}{2\Gamma}, \quad (30)$$

where T_K is the Kondo temperature given by Eq. (14). Then the linear conductance for $T < T_K$ is

$$G = \frac{\pi T_K G_0}{4T} \int \frac{d\epsilon \mathcal{S}_f(\epsilon)}{\cosh^2\left(\frac{\epsilon}{2T}\right)} \frac{(\Gamma_L + \Gamma_R) \text{Im}\chi(\epsilon)}{\Gamma_L + \Gamma_R \text{Im}\chi(\epsilon)}, \quad (31)$$

where

$$\mathcal{S}_f(\epsilon) = \frac{T_K \gamma(\epsilon)}{(\epsilon - \bar{\epsilon}_0)^2 + (T_K)^2 \gamma^2(\epsilon)},$$

$$\gamma(\epsilon) = \frac{\pi}{2} \frac{\Gamma_L + \Gamma_R \text{Im}\chi(\epsilon)}{\Gamma_L + \Gamma_R},$$

G_0 is given by Eq. (26), $\chi(\epsilon)$ is given by Eq. (17).

The zero bias conductance as a function of temperature is shown in Fig. 4 for $\nu = 0, 0.2T_K, 0.4T_K, 0.6T_K$ and $0.8T_K$. The temperature dependence of the conductance is similar to the one shown in Fig. 2 for $T > T_K$. In both cases, when $T > \nu$, a peak in the conductance occurs (see curves b, c, d and e). This peak decreases with ν and shifts towards high temperatures. For $T < \nu$, the conductance decreases with decreasing in T and vanishes when $T \rightarrow 0$. This is a manifestation of the coupling between the QSH states on the opposite sides of the TI. For $\nu = 0$, the conductance has a usual peak at $T = 0$.

Summary: The linear and non-linear conductance in a system consisting of a quantum dot (tuned to the Kondo regime) connected to a metal lead on the left side and to a topological insulator on the right side is evaluated using Keldysh technique. Renormalization group analysis is performed in the weak coupling regime ($T \gg T_K$) while the MFSBA is used at the strong coupling regime $T < T_K$. When the coupling energy ν between QSH helical states exceeds the temperature, the differential conductance develops a dip at low temperature, in contrast with the standard zero bias anomaly Kondo peak prevailing in QD connected to metallic leads. Our analysis then shows that the Kondo resonance is very sensitive to edge state coupling and can be used to probe the features of QSH helical modes.

Acknowledgment: We thank the Israeli Science Foundation for supporting our research under grant 1173/08.

¹ J.C.Y. Teo, C.L. Kane, Phys.Rev. **B 82**, 115120 (2010).
² A.P. Schnyder, S. Ryu, A. Furusaki, and A.W.W. Ludwig, Phys. Rev. B **78**, 195125 (2008).
³ A.P. Schnyder, S. Ryu, A. Furusaki, and A.W.W. Ludwig, AIP Conf. Proc. **1134**, 10 (2009).
⁴ C.L. Kane and E.J. Mele, Phys. Rev. Lett. **95**, 146802 (2005).

⁵ Liang Fu, C.L. Kane, and E.J. Mele, Phys. Rev. Lett. **98**, 106803 (2007).
⁶ M.Z. Hasan and C.L. Kane, Rev. Mod. Phys. **82**, 3045 (2010).
⁷ Liang Fu and C.L. Kane, Phys. Rev. B **76**, 045302 (2007).
⁸ Liang Fu and C. L. Kane, Phys. Rev. Lett. **100**, 096407 (2008).

- ⁹ D. Hsieh, Y. Xia, D. Qian, L. Wray, F. Meier, J.H. Dil, J. Osterwalder, L. Patthey, A.V. Fedorov, H. Lin, A. Bansil, D. Grauer, Y.S. Hor, R.J. Cava, and M.Z. Hasan, *Phys. Rev. Lett.* **103**, 146401 (2009).
- ¹⁰ T. Zhang, P. Cheng, X. Chen, J.-F. Jia, X. Ma, K. He, L. Wang, H. Zhang, X. Dai, Z. Fang, X. Xie, and Q.-K. Xue, *Phys. Rev. Lett.* **103**, 266803 (2009)
- ¹¹ Y.S. Hor, A. Richardella, P. Roushan, Y. Xia, J.G. Checkelsky, A. Yazdani, M.Z. Hasan, N.P. Ong, and R.J. Cava, *Phys. Rev. B* **79**, 195208 (2009).
- ¹² C.-X. Liu, X.-L. Qi, X. Dai, Z. Fang, and S.-C. Zhang, *Phys. Rev. Lett.* **101**, 146802 (2008).
- ¹³ N.H. Lindner, G. Refael and V. Galitski, *Nature Physics* **7**, 490 (2011).
- ¹⁴ J.G. Checkelsky, Y.S. Hor, M.-H. Liu, D.-X. Qu, R.J. Cava, and N.P. Ong, *Phys. Rev. Lett.* **103**, 246601 (2009).
- ¹⁵ M. König et al., *Science* **318**, 766, (2007).
- ¹⁶ R. Egger, A. Zazunov, and A. Levy Yeyati, *Phys. Rev. Lett.* **105**, 136403 (2010).
- ¹⁷ G. Tkachov, E. M. Hankiewicz, *Phys. Rev. B* **83**, 155412 (2011).
- ¹⁸ Y. Tanaka, T. Yokoyama, and N. Nagaosa, *Phys. Rev. Lett.* **103**, 107002 (2009).
- ¹⁹ H.-Z. Lu, W.-Y. Shan, W. Yao, Q. Niu, and S.-Q. Shen, *Phys. Rev. B* **81**, 115407 (2010).
- ²⁰ C. Timm, [arXiv:1111.2245](https://arxiv.org/abs/1111.2245).
- ²¹ A. Golub, I. Kuzmenko, and Y. Avishai, *Phys. Rev. Lett.* **107**, 176802 (2011).
- ²² Y. Okada, C. Dhital, Wen-Wen Zhou, Hsin Lin, S. Basak, A. Bansil, Y. -B. Huang, H. Ding, Z. Wang, Stephen D. Wilson, V. Madhavan, *Phys. Rev. Lett.*, **106**, 206805 (2011).
- ²³ C.-Y. Seng, T.-K. Ng, [arXiv 1012.5867](https://arxiv.org/abs/1012.5867).
- ²⁴ J.R. Schrieffer and P.A. Wolff, *Phys. Rev.* **149**, 491 (1966).
- ²⁵ **25** M. Pustilnik and L. Glazman, *Phys. Rev. Lett.* **85**, 2993 (2000); [cond-mat/0102458](https://arxiv.org/abs/cond-mat/0102458).
- ²⁶ **26** K. Kikoin, Y. Avishai, *Phys. Rev. B* **65**, 115329 (2002); [cond-mat/0107473](https://arxiv.org/abs/cond-mat/0107473).
- ²⁷ A. Kaminski, Yu. V. Nazarov, and L.I. Glazman, *Phys. Rev. B* **62**, 8154 (2000).